THE JOURNAL OF PHYSICAL CHEMISTRY C

Article

Cite This: *J. Phys. Chem. C* 2019, 123, 10225−10236

pubs.acs.org/JPCC

Low Internal Reorganization Energy of the Metal−Metal-to-Ligand Charge Transfer Emission in Dimeric Pt(II) Complexes

Wei-Chih Chen, Pi-Tai Chou, and Yuan-Chung Cheng*

Department of Chemistry, National Taiwan University, Taipei City 106, Taiwan

Supporting Information

ABSTRACT: To achieve near-infrared (NIR) emitters with high photoluminescence quantum yield, reduction of nonradiative decay is necessary. There, the energy gap law dictates that as the emission wavelength shifts to the red, the nonradiative decay of the excited state becomes more rapid, unless the vibronic couplings can be simultaneously suppressed. In this study, we apply density functional theory to investigate vibronic coupling effects in a series of high-efficiency square-planar Pt(II) emitters in both the monomeric and dimeric forms. We reveal that the magnitude of internal reorganization energy, which is a measure of the extent of intracomplex vibronic coupling between two electronic states, can be significantly reduced in the dimers by the formation of metal−metal-to-ligand-charge-transfer excimeric states on the lowest triplet excited-state potential energy surface, despite that in the monomer complexes the triplet state exhibits a mixed intraligand-charge-transfer/metal-to-ligand-charge-transfer character that leads to large reorganization energies. Furthermore, we demonstrate that the relative magnitudes of the reorganization energies and the ligand substituent effects can be fully rationalized using the transition density between the excited state and the ground state as a theoretical tool that represents the spatial distribution of excitations. Finally, we expand our calculations to 45 Pt(II) NIR emitters to show that internal reorganization energy is a key factor affecting the photoluminescence quantum yield, in accordance with the energy gap law. Our findings clearly elucidate the vibronic factors affecting nonradiative decays in molecular excited states and point to novel design principles for improved NIR emitters by controlling vibronic couplings through metallophilic interactions in molecular aggregates.

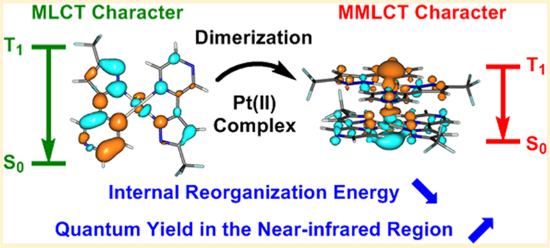

INTRODUCTION

Near-infrared (NIR) luminescent materials have found intensive research interest in many fields of science and technology.[1−5] In particular, phosphorescent transition-metal complexes with strong NIR emission have attracted much attention in recent years due to their long triplet lifetime and tunability with heterocyclic ligands and electron-donating/withdrawing substituent groups.[6−9] Nevertheless, it is still very challenging to develop complexes with high photoluminescence quantum yield (PLQY) in the NIR region because the small energy gap between the excited state and the ground state would accelerate the nonradiative decay of the excited state, as dictated by the energy gap law.[6] In this regard, Pt(II) complexes with excimer formation properties in the triplet excited state have become very promising NIR-emitting materials.[10−14] In aggregates or thin films, these square-planar complexes with proper ligand design have shown strong NIR emission from the lowest triplet excited state, which is assigned as a triplet metal−metal-to-ligand-charge-transfer (^{3}MMLCT) state. The ^{3}MMLCT character of dimeric Pt(II) complexes and their applications in novel supermolecular light emitters have been well documented.[15−17] However, previous studies mostly focused on the substituent effects on the electronic properties, and the factors controlling the PLQY remain unclear. In particular, the Pt(II) complexes with columnar-stacked structure in thin films exhibit emission wavelength at about 740 nm with PLQY as high as 81%.[18] The external quantum efficiency of up to 55% is also measured in organic light-emitting diode devices with out-coupling structures. The observed high PLQY in these NIR emitters indicates that the relationship between emission energy and quantum yield is highly nontrivial, and it is critical that the factors leading to the high PLQY in these Pt(II) complexes could be clearly elucidated.

According to the energy gap law,[19] the nonradiative decay process is controlled by the Franck−Condon overlap between the vibrational wave functions of the excited and the ground states. In the weak coupling limit, Fermi's golden rule yields a nonradiative vibronic transition rate as follows[19,20]

$$W = \frac{C^2\sqrt{2\pi}}{\hbar\sqrt{\hbar\omega_M \Delta E}} \exp(-\lambda_M/\hbar\omega_M) \exp\left\{-\frac{\Delta E}{\hbar\omega_M}\left[\log\left(\frac{\Delta E}{\lambda_M} - 1\right)\right]\right\}$$

where C is a coupling constant, ω_M is the frequency of the normal vibrations of maximum frequency, λ_M is the collective

Received: January 8, 2019
Revised: March 25, 2019
Published: April 1, 2019

DOI: 10.1021/acs.jpcc.9b00224
J. Phys. Chem. C 2019, 123, 10225−10236

reorganization energy of the maximum frequency modes, and ΔE is the energy gap between the two electronic states. The ΔE in the exponent predicts that the transition rate will increase exponentially as ΔE decreases, hence the energy gap law. The energy gap law is anticipated to be the major determinant in the efficiency of NIR emitters. Notably, the formula also predicts that in addition to the energy gap the nonradiative transition rate also depends on the mode frequency and the strength of vibronic couplings represented by the reorganization energy term. The lower the reorganization energy, the slower the transition rate will be. Note that this formula does not depend on the assumption of a single-frequency model; it is derived from the general many mode formula in the weak coupling limit because low-frequency modes will not contribute significantly to the vibronic transition rate due to their exponentially small Franck–Condon factors when the energy gap ΔE is relatively large.[19] Although general theoretical frameworks for full characterization of radiative and nonradiative decay processes in organometallic phosphors have been developed,[21−25] vibronic coupling effects have nevertheless been mostly overlooked in the rationales of efficient NIR emitter design in the past.[15−17] Conventionally, factors such as the molecular rigidity and delocalization length of the extended π-conjugated system have been used to implicate the strength of vibronic couplings;[26−30] however, these qualitative descriptors cannot provide a clear understanding of vibronic effects in nonradiative decay of molecular excited states. It is thus highly desirable to quantify vibronic couplings and their influences in nonradiative decay processes in NIR phosphors. In particular, it will be interesting to know how the different types of electronic transitions in square-planar Pt(II) complexes, such as the transformation from the mixed triplet intraligand-charge-transfer/metal-to-ligand-charge-transfer (^{3}ILCT/^{3}MLCT) state to the ^{3}MMLCT states by excimer formation, would have an impact on internal reorganization energy.

In this paper, we apply density functional theory (DFT) to investigate electronic properties and vibronic coupling effects in eight Pt(II) square-planar complexes (Figure 1). These complexes are chosen as our model systems because they have been synthesized before and were shown to exhibit remarkable NIR emission properties.[15,18,31,32] Moreover, these complexes can be regarded as derivatives of complex **1a** either by CF_3 substitution or by N-substitution, which provides an excellent setting for the investigation of substituent effects. Note that electronic properties and tunabilities of the S_1 and T_1 excitations in both the monomers and dimers of similar types of compounds have been studied in detail.[15,16] However, the trends in the observed PLQY especially the anomalously strong photoluminescence of the NIR emitters **1**−**3** in the solid states have never been clearly elucidated for the model compounds. Therefore, in this work, we focus on the vibronic coupling effects by calculating and analyzing reorganization energies of the triplet excitations of these Pt(II) complexes both in the monomeric and dimeric forms. Furthermore, we propose to use transition density as an effective theoretical tool to conceptualize vibronic coupling effects in molecular systems, and we adopt this tool to elucidate the key driver of nonradiative decay in NIR phosphors and to propose a new design principle for high-quantum-yield NIR emitters. This systematic analysis of the Pt(II) complexes should elucidate the molecular design principles that could be used to develop novel NIR phosphors. Thus, the key questions we aim to answer are as follows: (1) What are the factors leading to the red-shifted NIR photoluminescence emission in solid films of complexes **1b**, **2b**, and **3b**? (2) How the aggregation (dimerization) affects the electronic structures and vibronic couplings for low-lying excitations in these model compounds? (3) How can these systems achieve such high PLQYs despite the predictions of the energy gap law? Although partial answers to these questions have been presented in the literature, in this work, we aim to elucidate the full consequences of these intriguing questions.

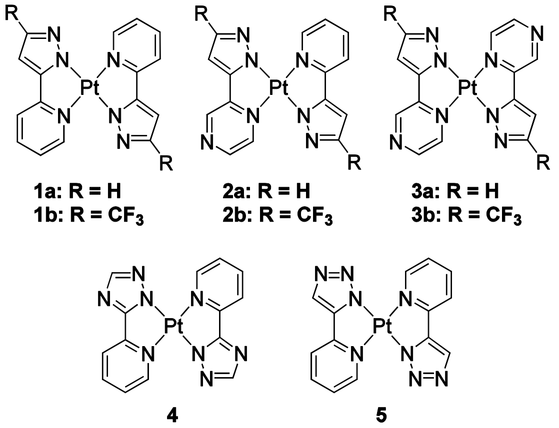

Figure 1. Chemical structures of the model Pt(II) complexes studied in this work. The model systems include the Pt(II) pyridyl pyrazolate complex (**1a**), N-substitution on pyridine ligands (**2a** and **3a**), N-substitution on pyrazole ligands (**4** and **5**), and the CF_3-substitution on the pyrazole ligands (**1b**, **2b**, and **3b**).

Note that in previous theoretical investigations of blue phosphorescent materials spin−orbit couplings have been considered to be important for the efficiency of the light emission.[21,23,24] Nevertheless, for the NIR phosphorescent systems studied in this work, nonradiative decay back to the ground state should be the dominant deactivation process. This is in contrast to the scenario in the blue phosphorescent systems, where the excited states have higher energies such that the relaxation back to the ground state is slower and might not be the dominant deactivation process. As a result, multiple decay channels could influence the excited-state dynamics and therefore large spin−orbit couplings and rapid intersystem crossing play important roles in the determination of the quantum yield of blue phosphorescent systems. Given that the spin−orbit couplings in platinum complexes should be sufficiently large to yield rapid intersystem crossing and that the vibronic couplings in dimer systems are rarely reported, we choose to first ignore the spin−orbit coupling effects and focus instead on the vibronic effects and the energy gap law in this work. As far as we are aware of, the reorganization energy for Pt(II) dimer systems and the different roles of intra- and intercomplex modes have never been investigated previously. The full characterization including the spin−orbit couplings and radiative decay constants will be carried out in a future study.

■ COMPUTATIONAL DETAILS

All calculations presented in this study were carried out using the Gaussian 09 program.[33] Here, the molecular geometries of the ground state (S_0) were optimized at the B3LYP-D3(BJ) level[34] because DFT methods with empirical dispersion correction have been shown to provide a better assessment of the intermolecular metal−metal and $\pi-\pi$ interactions.[35] The DFT methods have been shown to be reliable in obtaining the electronic properties of Pt(II) complexes.[13,16,36−39] The time-dependent density functional theory (TDDFT) with the Tamm−Dancoff approximation (TDA) and B3LYP-D3(BJ) functional, i.e., TDA-B3LYP-D3(BJ), is employed in the geometry optimization of the lowest singlet and triplet excited states (S_1 and T_1). The triplet instabilities in TDDFT, which would cause the underestimation of triplet excited state, can be alleviated by the TDA.[40,41] Furthermore, previous studies have shown that the TDA-DFT calculation results are in good agreement with the experimental phosphorescence emission energy of Pt(II) complexes.[38]

For all of the calculations, the effective core potential (ECP) LANL2DZ basis set for Pt atoms and the 6-31G(d,p) basis set for other atoms were used to investigate the optimized geometries and reorganization energies. Frequency analysis was performed to confirm that there is no imaginary frequency for all minimal geometries. Single-point calculations for the electronic properties were carried out with the SDD/6-311+G(d,p) basis set. In our study, the SDD ECP basis set yields more accurate emission energies for ^{3}MMLCT transitions due to the increasing orbital overlap between Pt atoms.

We note that M06-2X has been shown to yield better geometries for similar Pt(II) complexes.[25] Better geometries should yield improved results, and a benchmark study would be useful to determine the best functional and basis set for the systems studied in this work. However, given the complexities of the systems and their dependences on transition energy and solvent environments, it would be very challenging to exactly reproduce the experimental transition energies using DFT calculations. Since in this work we focus on trends in reorganization energies, which are calculated from relative energies, we believe that the B3LYP-D3(BJ) functional should yield adequate results.

The reorganization energy in the T_1 excited state is calculated on the adiabatic potential energy surface of the S_0 state (E_{S_0})[42,43]

$$\lambda_m = E_{S_0}(Q_{T_1}) - E_{S_0}(Q_{S_0})$$

where Q_{T_1} and Q_{S_0} represent the equilibrium structure of the T_1 and S_0 states, respectively. Therefore, $E_{S_0}(Q_{T_1}) - E_{S_0}(Q_{S_0})$ is the energy difference between the equilibrium T_1 and S_0 structures on the S_0 state energy. For all of the Pt(II) complexes, we calculate reorganization energies for both the monomers (λ_m) and dimers (λ_d).

To further characterize the excimerization process, the reorganization energy for a dimer (λ_d) is further decomposed into the internal and intercomplex reorganization energies, denoted λ_{in} and λ_{ic}, respectively. We consider λ_{in} as the part of the reorganization energy contributed by structure distortions localized on a single monomeric subunit upon T_1 excitation in a dimeric complex. Therefore, we perform geometry optimization for the dimeric complex in the T_1 excited state and then take the structure of one of the monomeric subunits to calculate its S_0 energy. This S_0 energy is then compared to the equilibrium S_0 energy to obtain the internal reorganization energy per monomer, λ_{in}. Once λ_{in} is obtained, the intercomplex reorganization energy can be calculated using

$$\lambda_{ic} = \lambda_d - 2\lambda_{in}$$

Finally, the molecular reorganization energy can be partitioned into contributions from each normal mode to map out mode-specific vibronic couplings[42−44]

$$\lambda = \sum_{j}^{3n-6} \lambda_j = \sum_{j}^{3n-6} \hbar\omega_j S_j$$

$$S_j = \frac{1}{2\hbar}\omega_j d_j^2$$

where S_j is the Huang−Rhys factor describing the vibronic coupling between the T_1 state and the S_0 state for the jth ground-state normal mode and d_j is the displacement between the equilibrium structure of the T_1 and S_0 states.

RESULTS AND DISCUSSION

Electronic and Emission Properties of Pt(II) Complexes. To elucidate the electronic properties of the monomeric Pt(II) complexes, we calculated the T_1-optimized geometries and electronic properties at the equilibrium structures. Figure 2 shows the frontier orbitals of the model complexes **3a** and **5**. The orbitals for all of the complexes studied in this work are depicted in Figure S1. Generally speaking, these complexes exhibit similar lowest unoccupied molecular orbital (LUMO) patterns, whereas the highest occupied molecular orbitals (HOMOs) are strongly dependent on the molecular framework and substituents on the ligands. All of the frontier orbitals are dominated by the ligand orbitals, with the HOMOs showing more Pt contribution. Mulliken population analysis reveals that the HOMO and LUMO populations on the Pt atom are 10−32 and 3−4%, respectively.

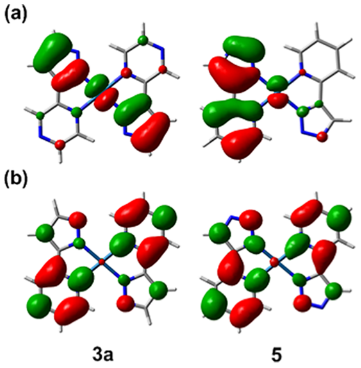

Figure 2. (a) HOMO and (b) LUMO of Pt(II) complexes **3a** and **5** in the T_1 equilibrium geometry.

To investigate the emission from the T_1 excited state and the substituent effects that might cause different electronic emission properties, the calculated emission wavelengths and characters of the Pt(II) monomer complexes in the T_1 state are listed in Table 1. The dominant T_1 configuration is the HOMO-to-LUMO transition. Since the HOMO contains more Pt contribution, the excitation is consistent with the triplet intraligand-charge-transfer/metal-to-ligand-charge-transfer (^{3}ILCT/^{3}MLCT) character, in agreement with previous studies. For the substituted pyrazolate Pt(II) complexes (**1b**, **2b**, **3b**, **4**, and **5**), the HOMO-to-LUMO transition accounts for 75.5−84.9% of the total contribution, which is obviously lower than that for the unsubstituted complexes. This substitution effect is due to the interaction with the HOMO

Table 1. Emission Properties and Reorganization Energies in the T_1 State of Pt(II) Complexes

Pt(II) complex	λ_{em}[a] (nm)	transition configuration[b]	λ_m[c] (meV)	$\Delta E_{S_1-T_1}$[d] (eV)
1a	540	HOMO(32%) → LUMO(3%) 94.8%	178	0.22
1b	513	HOMO(25%) → LUMO(4%) 75.5%	233	0.26
2a	622	HOMO(31%) → LUMO(4%) 94.1%	236	0.19
2b	565	HOMO(26%) → LUMO(4%) 77.5%	216	0.23
3a	623	HOMO(30%) → LUMO(3%) 95.7%	184	0.18
3b	569	HOMO(24%) → LUMO(3%) 79.9%	194	0.21
4	543	HOMO(26%) → LUMO(4%) 84.9%	228	0.31
5	504	HOMO(10%) → LUMO(4%) 78.7%	264	0.37

[a]Emission wavelength. [b]In the parentheses are contributions of d orbitals of Pt atoms. [c]Reorganization energy of the Pt(II) monomer complex. [d]Energy gap between the S_1 and T_1 states.

− 1 orbital. According to the orbital-interaction theory,[45] the addition of electron-withdrawing groups stabilizes the orbital energy, especially when the substitution is on the non-nodal positions. The introduction of the N atom or CF_3 group to the pyrazolate unit thus lowers the HOMO energy significantly because the HOMO has large amplitudes on the pyrazole ring. This reduces the energy gap between HOMO and HOMO − 1, leading to mixing of the HOMO → LUMO and HOMO − 1 → LUMO configurations. Therefore, for the substituted pyrazolate Pt(II) complexes, additional single-excitation configurations are mixed into the T_1 state and the electron population on the Pt atom is decreased compared to the complex **1a**.

The emission energy is also tunable by the substituents in these Pt(II) complexes. For example, from complex **1a** to **2a** and to **3a**, the emission energy undergoes a red shift from 540 to 622 and to 623 nm because N-substitution in the pyridyl units stabilizes the energy of LUMO more than HOMO. This is explained by the larger pyridyl contribution in the LUMO (Figure 2). In contrast, the CF_3 substitution on the pyrazolate units more strongly stabilizes the HOMO energy because HOMO has more amplitudes on the pyrazolate units compared to the LUMO. As a result, CF_3-substituted complexes (**1b**, **2b**, and **3b**) exhibit blue-shifted emission relative to the unsubstituted complexes. Note that although these CF_3-substituted complexes present blue-shifted emission, the CF_3 group provides more ordered aggregations in the solid films,[31,32] which is advantageous. Obviously, the ligand design should take into account both tunable emission energy and molecular packing in exploring high-efficiency NIR phosphors.

Reorganization Energies of Pt(II) Complexes. To investigate vibronic effects, the reorganization energy of the monomeric T_1 state is also calculated and listed in Table 1. The data indicate that although the molecular rigidity and size of the π-conjugated system are similar among these Pt(II) complexes, the value of the monomer reorganization energy (λ_m) can vary significantly by up to 86 meV. Furthermore, λ_m is decomposed into the contributions from specific normal modes (Figures 3 and S2). For the Pt(II) complexes studied in this paper, the vibration modes below 700 cm^{-1} are mostly Pt−N vibrations and the C−C, C−N, and N−N vibrations in the ligands occur at 700−1600 cm^{-1}. This is in agreement with experimental results indicating that metal−ligand vibrations in transition-metal complexes are low-frequency modes.[46,47] Figure 3 shows that modes with significant vibronic couplings are predominantly high-frequency ligand modes. Therefore, mode-specific reorganization energy indicates that the dominant contribution of vibronic effects comes from the ligand vibrations and therefore the various ligand substituents should have a significant impact on the vibronic couplings.

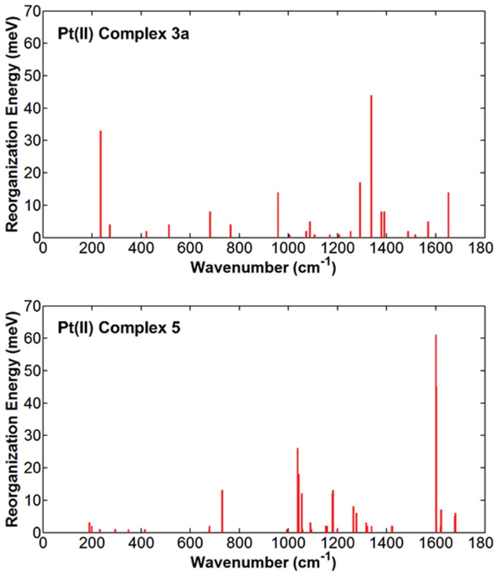

Figure 3. Mode-specific reorganization energy of Pt(II) complexes in the T_1 excited state. The stick diagram shows the single-mode reorganization energy at different vibration frequencies.

Our calculations also reveal that N-substitution in the pyridyl unit (**1a** → **3a**) and N-substitution in the pyrazolate unit (e.g., **1a** → **5**) show drastic differences in the change of λ_m. λ_m for **3a** is not very different from that of **1a**, whereas λ_m of complex **5** is significantly higher. The strong substituent effects on λ_m cannot be easily rationalized. To address this issue and furthermore predictively determine the relative strengths of vibronic couplings, we need to go beyond the traditional molecular rigidity description of the molecular reorganization energy. It is thus highly desirable to develop an intuitive way to understand the various substituent effects on molecular reorganization energy to explain the difference in λ_m between the Pt(II) complexes **3b** and **5**. To this end, we extend an orbital-interaction rule in the rationalization of substituent effects on the reorganization energy of charge transfer processes. In the charge transfer case, how substituents affect the magnitude of reorganization energy can be estimated from the pattern of the molecular frontier orbitals by regarding the LUMO (HOMO) approximately as the electron (hole) distribution.[48,49] As a result, when an electron (hole) is added into the molecule, the bond length strongly changes at the locations where the two atoms exhibit strong bonding or antibonding character in the LUMO (HOMO).[50] Therefore, substitutions at the positions where the HOMO/LUMO has strong bonding or antibonding characters would more significantly affect the reorganization energy. In contrast, substitutions at the positions with local nonbonding character in frontier orbitals will not affect the reorganization energy.[51−53] This finding provides a powerful way to elucidate the dependence of reorganization energy on the molecular structure in charge transfer processes. However, a single molecular orbital cannot characterize an electronic transition from the ground state to the excited state. For molecular excited states, the transition density between two electronic states should provide a suitable description of the spatial distribution of excitation.[54]

To explore the effectiveness of using transition density as a theoretical tool to understand the vibronic couplings in molecular excitations, we investigate the correlation between the distribution of transition density and the structural distortions in the T_1 excited state of the model Pt(II) complexes (Figures 4 and S4). In Figure 4a, we show the transition density of three model compounds. Among these Pt(II) complexes, the transition density between the T_1 and S_0 states is primarily the product of the HOMO and LUMO orbital wave functions. The transition density of complex **3a** is distributed evenly on the four ligand units. In contrast, the transition density of complex **5** is localized on one side, i.e., the ligand units B and D. We expect that the drastically different distributions of the transition densities will give rise to different structural distortions for complexes **3a** and **5**. Indeed, the bond-length differences between the T_1 and S_0 states as shown in Figure 4b exhibit strong spatial correlation with the distribution of transition densities. The four-ligand regions show similar average absolute bond-length differences for complex **3a**, just like the evenly distributed transition density. In contrast, the transition density of complex **5** is localized on the ligand regions B and D, and it is not surprising that bond-length differences in the T_1 state appear only in these two regions. It is also clear that neighboring atoms with bonding or antibonding characters in the transition density show more dramatic bond-length differences in the excited state, as evidenced in the variations in the bond-length differences of selected bonds shown in Figure 4b. Clearly, transition density provides a map for structure distortions upon excitation into an electronically excited state.

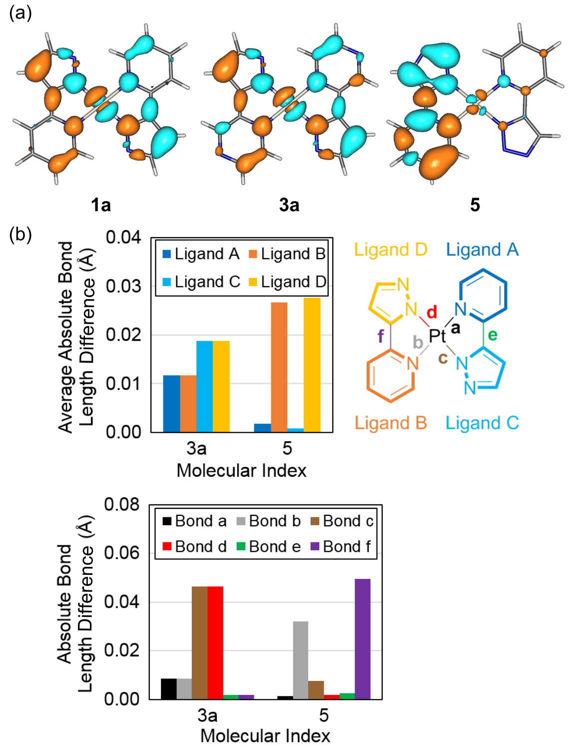

Figure 4. (a) Transition density and (b) absolute bond-length alterations between the T_1 and S_0 states of Pt(II) complexes **3a** and **5**.

Furthermore, the strong correlation between the spatial distribution of transition density and the bond-length differences suggests that the transition density could be employed as a theoretical measure to determine substituent effects in the vibronic couplings. We expect that substitution at a position with strong bonding or antibonding character with its neighbors in the transition density will strongly affect the reorganization energy of the excitation, whereas substitution at a position not interacting with its neighbors in the transition density will have negligible effects on the reorganization energy. To rationalize the different λ_m values for complexes **3a** and **5**, we now consider the transition density of complex **1a** shown in Figure 4a. It is quite clear that the small reorganization difference between complexes **1a** and **3a** can be rationalized because the substitution on the pyridyl unit is at a position with weak bonding/antibonding character in the transition density, whereas from **1a** to **5**, the substitution on the pyrazolate unit is at a position of strong bonding/antibonding character in the transition density, leading to the significant increase in the reorganization energy. In summary, the substitution effects on the reorganization energies of electronically excited states can be explained by the pattern of the transition density. We believe that this is for the first time that the structural distortions and substituent effects in tuning the strengths of vibronic couplings in the excited states can be fully rationalized. By inspecting the pattern of the transition density, one can determine how substituents would affect the magnitude of reorganization energy. Since it is advantageous to avoid making significant increases in the reorganization energy as the electronic excitation properties are tuned in developing new materials for many optoelectronic applications, substitution at the nodal position of the transition density should be considered an effective strategy to achieve this goal.

Optimized Geometries in the T_1 and S_0 States of Dimeric Pt(II) Complexes. The calculations of electronic properties and reorganization energies were also performed for the dimeric Pt(II) complexes of the model compounds. Here, we first examine the optimized structure of dimers, which should have significant impacts on the electronic structures and emission properties. The equilibrium geometries of the dimeric Pt(II) complexes at the S_0 and T_1 states are summarized in Table 2. For the dimers in the ground state, the Pt−Pt (3.19−3.31 Å) and ligand−ligand (3.08−3.25 Å) distances are slightly smaller than the sum of the van der Waals radii of Pt atoms (3.50 Å) as well as the common $\pi-\pi$ distance (3.40 Å). Therefore, the intercomplex binding energy in the dimers contains both metallophilic and interligand interactions. The analysis of the composition of dispersion energy for π-stacked d^8 metal complexes has demonstrated that the ligand−ligand interactions are the dominant contribution to the binding energy in S_0.[17,55] For the model dimeric Pt(II) complexes studied in this work, the dimer formation in the S_0 state is affected by the substituents on the ligands. The molecular

Table 2. Optimized Geometries in the T_1 and S_0 States of Dimeric Pt(II) Complexes

	S_0				T_1			
dimeric Pt(II) complex	d_M[a] (Å)	d_L[b] (Å)	d_{xy}[c] (Å)	θ[d] (deg)	d_M (Å)	d_L (Å)	d_{xy} (Å)	θ (deg)
$(\mathbf{1a})_2$	3.22	3.18	0.00	50.8	2.83	3.14	0.01	31.0
$(\mathbf{1b})_2$	3.28	3.13	0.15	23.7	2.84	3.06	0.08	25.6
$(\mathbf{2a})_2$	3.20	3.18	0.09	52.9	2.83	3.13	0.09	30.9
$(\mathbf{2b})_2$	3.30	3.12	0.03	21.8	2.84	3.06	0.03	24.4
$(\mathbf{3a})_2$	3.19	3.17	0.00	54.7	2.83	3.11	0.00	31.0
$(\mathbf{3b})_2$	3.31	3.12	0.04	21.4	2.84	3.04	0.02	23.5
$(\mathbf{4})_2$	3.23	3.25	0.01	103.2	2.84	3.20	0.00	97.9
$(\mathbf{5})_2$	3.27	3.08	0.27	42.6	2.83	3.07	0.00	29.3

[a]Pt–Pt distance. [b]Average ligand–ligand distance. [c]Projected distance between the two Pt atoms in the *xy*-plane [d]Dihedral angle between two monomer complexes as shown in Figure 5.

frameworks with C_{2h} symmetry, where the center of mass is located on the Pt atom, tend to balance each interligand interactions and then constrain the movement on the *xy*-plane. Therefore, the metals are readily oriented along the *z* axis in the optimized structures. On the other hand, when the negative charge of the π-cloud is strongly induced on the ligands [e.g., $(\mathbf{5})_2$], the electrostatic interactions make the Pt atom to be slightly shifted away from the *z* axis (Figure S6).

For dimers in the T_1 state, the Pt–Pt distances are significantly shortened to 2.83–2.84 Å, which are in agreement with similar Pt(II) complexes observed in experiments.[56−60] On the other hand, the π–π interactions in the excited state slightly reduce the average ligand–ligand distances to 3.04–3.20 Å. For the dimers in the excited state, the Pt–Pt distance is smaller than the ligand–ligand distances. As a result, we identify the key driving force of dimerization as the Pt d_z^2–d_z^2 interactions in the excited state, which is clearly demonstrated in the excimer structures. Moreover, as shown in Figure 5, π–π interactions between monomers in the excited state have a stronger impact on relative rotational angle θ, especially for the Pt(II) complexes without CF_3 substituents. Overall, our calculations confirm effective excimer formation in the T_1 excited state.[15−17] It is worth noting that the Pt(II) complexes $(\mathbf{1b})_2$, $(\mathbf{2b})_2$, and $(\mathbf{3b})_2$ exhibit high PLQY in experiments and their equilibrium structures in the solid state for the T_1 and S_0 states are very similar. Therefore, efficient formation of triplet excimers in solids should play a crucial role in this kind of NIR materials.

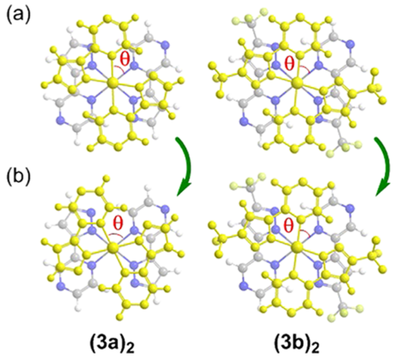

Figure 5. Optimized geometries of dimeric Pt(II) complexes $(\mathbf{3a})_2$ and $(\mathbf{5})_2$ in the (a) T_1 and (b) S_0 states.

Electronic and Emission Properties of Dimeric Pt(II) Complexes. In Figure 6, the frontier orbitals of the representative dimeric Pt(II) complexes are shown (also see Figure S4). The HOMOs of the dimer are drastically different from those of the monomers (Figures 2 and S1). Because of the short intercomplex distance due to the strong metallophilic interactions between the two Pt atoms, the strong d_{z^2}–d_{z^2} interactions raise the energy of the occupied $\sigma_d z^{2*}$ orbital, making it become the HOMO in the dimers. On the other hand, the LUMO of the dimeric complexes is formed by the π–π bonding interaction between the individual LUMOs of the two monomers. Therefore, the electronic distributions of HOMO and LUMO are mainly located on the two Pt atoms and the ligands, respectively. The electronic distribution of the frontier orbitals also indicates that the electron-withdrawing groups on the ligands play a more significant role in tuning the energy level of the LUMO rather than that of the HOMO.

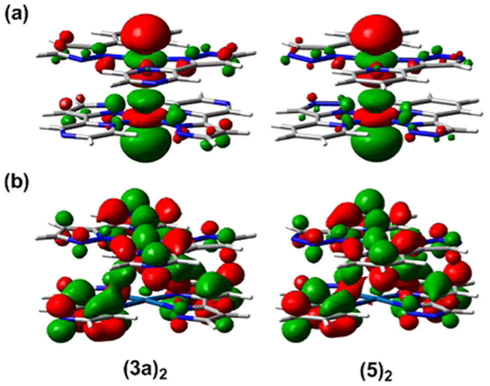

Figure 6. (a) HOMO and (b) LUMO of Pt(II) dimeric complexes $(\mathbf{3a})_2$ and $(\mathbf{5})_2$ in the T_1 state.

The emission properties of the dimeric Pt(II) complexes in the T_1 state are presented in Table 3. The dimeric emission wavelengths are strongly red-shifted with respect to those of the monomers. This is expected as the triplet excimer formation in the dimeric Pt(II) complexes would significantly lower the energy of the T_1 state. Furthermore, we confirm that the T_1 state exhibits HOMO-to-LUMO transition up to 99% and thus can be assigned as a ^{3}MMLCT state. Upon excitation, depopulation from the HOMO, which has the $\sigma_d z^{2*}$ antibonding character, would significantly enhance the attractive interaction between the Pt atoms, resulting in the formation of an excimeric state and shortened Pt–Pt distance. Excimer formation in ^{3}MMLCT excited states was quite well recognized in the literature.[16]

Considering the substituent effects, the emission wavelengths in excimers exhibit the same trend as the one found in the monomers, except for the $(\mathbf{4})_2$ complex. We found that this

Table 3. Emission Properties and Reorganization Energies in the T_1 State of Dimeric Pt(II) Complexes

dimeric Pt(II) complex	λ_{em}[a] (nm)	transition configuration[b]	λ_{d}[c] (meV)	λ_{in}[d] (meV)	λ_{ic}[e] (meV)	$\Delta E_{S_1-T_1}$[f] (eV)
(1a)$_2$	692	HOMO(83%) → LUMO(5%) 99.1%	371	39	294	0.18
(1b)$_2$	664	HOMO(84%) → LUMO(5%) 99.1%	329	37	256	0.18
(2a)$_2$	766	HOMO(82%) → LUMO(5%) 99.2%	424	45	333	0.17
(2b)$_2$	724	HOMO(83%) → LUMO(5%) 99.1%	333	31	271	0.18
(3a)$_2$	794	HOMO(81%) → LUMO(4%) 99.2%	446	43	361	0.18
(3b)$_2$	759	HOMO(83%) → LUMO(5%) 99.2%	327	25	278	0.18
(4)$_2$	632	HOMO(85%) → LUMO(5%) 99.0%	325	56	213	0.19
(5)$_2$	652	HOMO(85%) → LUMO(6%) 99.0%	366	38	291	0.19

[a] Emission wavelength. [b] Contributions of d orbitals of Pt atoms in parentheses were calculated by natural bonding orbital analysis. [c] Reorganization energy of the Pt(II) dimeric complex. [d] Internal reorganization energy of the Pt(II) dimeric complex. [e] External reorganization energy of the Pt(II) dimeric complex. [f] Energy gap between the S_1 and T_1 states.

is due to its significantly different molecular packing in the T_1 state (Figure S5). The weak $\pi-\pi$ bonding interaction between the LUMOs of the two monomers slightly lowers the LUMO energy of the dimer and causes the emission wavelength of the dimeric Pt(II) complex **(4)**$_2$ to be strongly blue-shifted compared to other dimers. The collective data indicate that to have efficient and deep-red NIR emission from the ^{3}MMLCT state the proper ligand design should also consider the control of the molecular packing so that the intercomplex interactions can be adjusted properly.[61]

Reorganization Energies of Dimeric Pt(II) Complexes. Now, we shift our focus to vibronic effects in the dimeric Pt(II) complexes. Considering the excimeric character of the ^{3}MMLCT excited state of the dimeric Pt(II) complexes, the vibronic couplings as well as the reorganization process are expected to be drastically different from those in the monomers. This is consistent with the experimental observation that the emission properties of the Pt(II) complexes in the solution (monomer) and the aggregates/solids (dimer) are markedly different.[15−17,31,59] Note that the term excimer is loosely applied to describe strongly enhanced intercomplex interactions in the excited states. We expect that upon photoexcitation into the allowed S_1 excited state and the subsequent rapid intersystem crossing to the T_1 state the Pt−Pt distance would shorten to stabilize the T_1 state and destabilize the S_0 state. Thus, this excimerization process would lead to significantly red-shifted photoluminescence emission. Although the excimer formation is expected to contribute to a major part of the reorganization energy in the T_1 state, the intercomplex motions involve extremely low frequency modes. According to the energy gap law, nonradiative decay mediated by these modes would be very inefficient because of the large number of vibrational quanta involved in the process (i.e., small Franck−Condon factor). It is thus a good approximation to assume that the intercomplex modes do not contribute to the nonradiative decay and the decay of the excited state is driven mainly by the high-frequency intracomplex vibrations. We use the term internal reorganization energy to refer to the sum of the reorganization energies contributed by the intracomplex vibrations, and we suggest that the internal reorganization energy makes a proper measure of the extent of vibronic couplings relevant to nonradiative decay in these dimeric complexes.

In Table 3, we show the dimer reorganization energy (λ_d) as well as its division into the internal (λ_{in}) and intercomplex (λ_{ic}) components. The results indicate that although the dimeric complexes exhibit a large overall reorganization energy λ_d the internal reorganization energy λ_{in} is significantly reduced in comparison to the monomer values. The striking difference in the magnitudes of λ_{in} and λ_{ic} in the dimeric Pt(II) complexes can be rationalized by the spatial distribution of the transition density of the ^{3}MMLCT excited state (Figures 8a and S7). Note that the substitutions on the ligands only slightly perturb the electronic distribution in the HOMO and LUMO, so the transition density of the ^{3}MMLCT excited state shows the similar spatial distribution for all of the dimeric Pt(II) complexes studied in this work. The ^{3}MMLCT transition density is mainly localized on the two Pt atoms, and hence λ_d is dominated by the intermolecular vibrations modulating the Pt−Pt distance. The large λ_{ic} is clearly dominated by the excimer formation process. Note that λ_{ic} includes the contributions from both the translational and rotational modes between the monomers, which are coupled to each other and difficult to separate. Nevertheless, we found that the substituent effects in λ_{ic} are correlated with the rotational angle θ between the optimized structures in the T_1 and S_0 states. We suspect that the translational contributions to λ_{ic} among these dimeric Pt(II) complexes are very similar. Therefore, as the rotational motion on the *xy*-plane is constrained in the excited state, such as the Pt(II) complexes **(1b)**$_2$−**(3b)**$_2$ and **(4)**$_2$, the λ_{ic} could be significantly reduced. Note that our dimer model is minimal and does not include spatial confinement effects due to steric/packing in molecular aggregates. Hence, the calculated λ_{ic} might not be representative of the intercomplex reorganizations in the real materials. Therefore, controlling the crystal packing of the Pt(II) complexes in the ground state is also an important issue.

On the other hand, the ^{3}MMLCT transition density shows only minor contributions from the ligand orbitals. Hence, λ_{in} is much smaller than λ_{ic}. The decomposition of λ_{in} into mode-specific contributions provides further evidence that high-frequency intraligand vibrations give rise to only a small fraction of λ_{in} and that the frequencies of the modes strongly coupled to the dimeric ^{3}MMLCT excitation are below 700 cm^{-1} (Figure 7), which should correspond to Pt−N bond stretching and bending modes. Moreover, the bond-length differences between the T_1 and S_0 states are negligible on the ligands (Figure 8). Therefore, the internal reorganization energy is significantly reduced in the ^{3}MMLCT excimeric state because of the small transition density distribution on the ligands. For the dimeric Pt(II) complexes studied in this work, the values of λ_{in} are below 60 meV, which are at least 3 times smaller than λ_m of the corresponding monomer. This is expected as the transition density of the ^{3}ILCT/^{3}MLCT state is mainly contributed by the ligands (Figure S3); the emission originating from the monomer generally leads to much higher

DOI: 10.1021/acs.jpcc.9b00224
J. Phys. Chem. C 2019, 123, 10225−10236

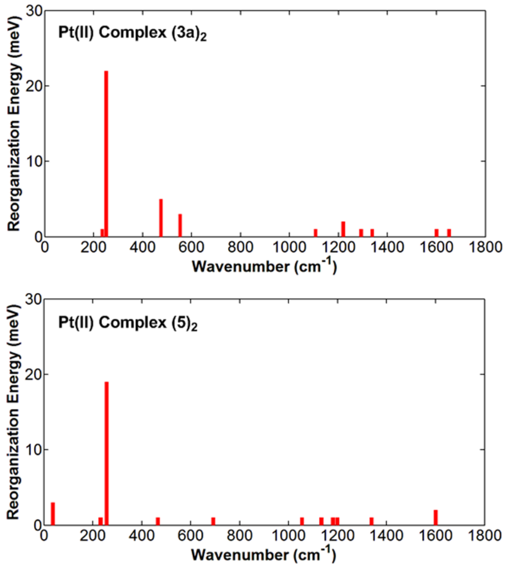

Figure 7. Mode-specific reorganization energy of dimeric Pt(II) complexes in the T_1 excited state. The stick diagram shows the single-mode reorganization energy at different vibration frequencies.

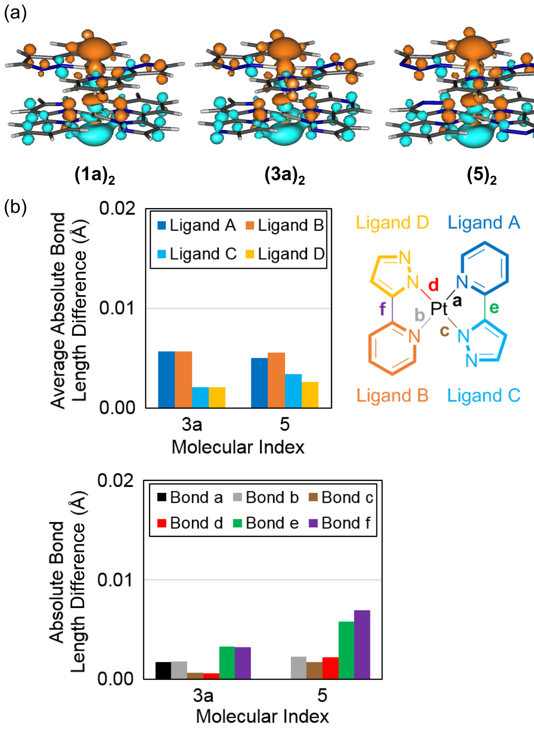

Figure 8. (a) Transition density and (b) absolute bond-length alterations between the T_1 and S_0 states of dimeric Pt(II) complexes $(\mathbf{3a})_2$ and $(\mathbf{5})_2$.

λ_m. As a result, the diminishing contribution of the vibronic couplings from the high-frequency ligand modes in the dimeric complexes is facilitated by the MMLCT character of the excited state. Therefore, the extent of vibronic couplings relevant to nonradiative decay is strongly suppressed in the dimers, leading to the high PLQY even when the emission is in the NIR region.

Internal Reorganization Energy and PLQY. The overall data presented in this work indicate that the internal reorganization energy for aggregates and monomers (for a single complex, $\lambda_{in} = \lambda_m$) is a useful measure for the strength of vibronic couplings driving nonradiative decay in the excited state. To verify this observation, we have identified 45 Pt(II) complexes with emission wavelength >625 nm in two review articles[6,17] and calculated λ_{in} for these systems. In Figure 9, we plot the emission wavelength and PLQY of these complexes while using colormap to present the calculated internal reorganization energy. We use the same level of theory in all calculations shown in Figure 9, and the full data set is given in Table S1. Clearly, the results show a strong correlation between the experimental PLQY value and the calculated λ_{in}. λ_{in} values for many complexes are above 200 meV, and they all exhibit negligible PLQY in the NIR region. Among them are Pt(II) complexes with mixed ^{3}ILCT/^{3}MLCT character in the T_1 state. On the other hand, strong emitters in the NIR region (>750 nm) all exhibit a λ_{in} that is below 100 meV. These results indicate that suppression of internal reorganization energy is necessary to achieve high-efficiency emitters in the NIR region, in accordance with the energy gap law. In particular, the porphyrinoid systems, which are well known for their small reorganization energies, exhibit high PLQY in the NIR region. Together with the ^{3}MMLCT dimer complexes studied in this work, these systems with small λ_{in} show a general trend in good agreement with the energy gap law: as the emission energy decreases, the PLQY decreases almost linearly. The results indicate that the energy gap and internal vibronic couplings are the two major determinants of the PLQY of NIR emitters. In the end, the energy gap law still holds; however, it is necessary to consider the microscopic details of the vibronic couplings. Note that although the energy gaps and reorganization energies generally explain the trends in the correlation between the PLQY and the emission energy shown in Figure 9 the dependence is only qualitative. It is also clear that future studies should include additional calculations such as spin−orbit couplings and radiative decay rates to achieve a full quantitative understanding of the quantum yields of these NIR emitters.

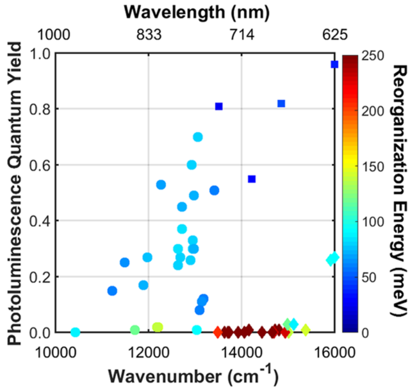

Figure 9. Experimental emission wavelength, photoluminescence quantum yield, and calculated internal reorganization energy of a collection of 45 Pt(II) complexes. Different symbols indicate different T_1 characters: the T_1 state with ^{3}MLCT/^{3}ILCT character (◊), the T_1 state with ^{3}MMLCT character (□), and complexes with porphyrinoid ligands (○).

Molecular Alignment and Delocalization Effect. It is worth to note that since the transition density of the ^{3}MMLCT state in the dimeric Pt(II) complexes studied in this work mainly originates from the d_{z^2} orbitals the excited-state properties should strongly depend on the relative orientation and positions of the two Pt atoms. An intercomplex displacement in the *xy*-plane would very effectively decrease the overlap between the two Pt d_{z^2} orbitals; hence, the energy level of the $\sigma_{dz^2}{}^*$ molecular orbital and the electronic transition character of the T_1 state could be easily affected by the molecular misalignments. We expect that a displacement in the *xy*-plane would result in mixing of d_{xz} and d_{yz} as well as the ligand orbitals in the HOMO, therefore leading to larger λ_{in} arising from the ligand vibrations.

In this work, we emphasize the drastic effect of dimerization on the electronic structures and vibronic couplings of the ^{3}MMLCT Pt(II) complexes and the dimerization as an effective means to significantly shift the emission to red while still keeping the nonradiative decay rate small by simultaneously suppressing the vibronic couplings of the internal vibrational modes. Another important point to be noted is that our dimer calculations represent only the minimal model to describe the electronic properties of the aggregates. In solid crystals or thin films, the intermolecular geometry is not determined simply by the pairwise interactions and the interacting molecular units could be much more extended (often extended over many molecules along a pseudo-1D direction). For the Pt(II) complexes studied here, the molecular alignment along the z axis would lead to strong excitonic coupling between complexes and thereby the photoexcitation is expected to be effectively delocalized among more than two molecules, forming an exciton. As the exciton delocalization length exceeds two molecules, λ_{in} can be significantly reduced.[62] Moreover, the energy gap between the T_1 and S_1 states, $\Delta E_{S_1-T_1}$, is expected to decrease as the exciton delocalization length increases because the exchange interactions in the more delocalized state will be diminished. Therefore, delocalized excitons in transition-metal aggregates could also be advantageous for enhancing radiative decays. In this regard, we must be cautious about comparing the results obtained from dimer calculations with experimental data and avoid overstating the impact of the dimer model. Nevertheless, we believe that we still gain valuable insights by investigating simplified dimer models.

■ CONCLUSIONS

In this paper, we apply density functional theory to investigate vibronic coupling effects in a series of square-planar Pt(II) complexes that showed promising NIR emission properties in the solid state. We show that the monomeric form of these transition-metal complexes shows mixed ^{3}ILCT/^{3}MLCT character in the T_1 state, which exhibits molecular reorganization energy ranging from 178 to 264 meV. To rationalize the substituent effects in the reorganization energies, we introduced the transition density between two electronic states as a theoretical tool to describe the spatial distribution of excitations and demonstrated that the structural distortion of the excited state relative to the ground state is strongly correlated with the spatial distribution of the transition density. Hence, the significant reorganization energy of the ^{3}ILCT/^{3}MLCT excited state is attributed to the large contribution of the ligand orbitals in the transition density, which causes strong vibronic couplings to the stretching modes in the ligand skeleton.

Furthermore, we calculated emission properties and reorganization energies for dimers of the model Pt(II) complexes. We confirmed excimer formation and the ^{3}MMLCT character of the T_1 excited state for the dimeric Pt(II) complexes. The strongly red-shifted emission is thus explained by the excimerization process and the destabilization of the metal–metal $\sigma_{dz^2}{}^*$ HOMO energy. To rationalize the high PLQY in the dimeric states, we follow the guidance of the energy gap law to divide the overall reorganization energy into a low-frequency intercomplex part and a high-frequency internal part. Although the low-frequency intercomplex reorganization energy due to the excimer formation contributes to a significant portion of the red shift in the triplet emission, it should play a negligible role in the nonradiative decay process. The internal reorganization energies for the dimers, however, are significantly reduced with respect to the monomer values. This result clearly explains the high PLQY of the dimeric ^{3}MMLCT excitations. The small internal reorganization energy in the excimeric state is also explained by the almost vanishing transition density on the heterocyclic ligands in the ^{3}MMLCT state. Because the transition density of the ^{3}MMLCT state is mainly localized on the two Pt atoms, the bond-length differences on the ligands become negligible.

To confirm the effectiveness of using the internal reorganization energy to quantify the strength of vibronic couplings driving nonradiative decay of excited states, we demonstrated a strong correlation between the experimental PLQY value and the calculated internal reorganization energy for 45 Pt(II) complexes found in the literature. This result strongly indicates that the reduction of the internal reorganization energy should be considered as a critical factor for improving the performance of NIR emitters.

In summary, this study not only clearly elucidated the factors leading to the red-shifted NIR photoluminescence emission in solid films of Pt(II) complexes studied here but also provided a rationale to understand the high PLQY found in some ^{3}MMLCT excited states. Furthermore, we emphasize that the spatial distribution of the transition density of the excited state could be utilized to design functionalized molecules with minimal λ_{in}. Our results suggest several additional key design principles besides the reduction of internal reorganization energy. In particular, transition-metal complexes preferentially aligned along the d_{z^2}-direction in crystal packing would be beneficial for light-emitting applications because in this case the internal reorganization energy can be greatly reduced due to the lowest-energy excited state associated with the electronic transition from metal $\sigma_{dz^2}{}^*$ to ligand π orbitals. It is worth mentioning that the σ^* interaction between d_{z^2} orbitals of transition metals strongly depends on the intercomplex distance, so the ligand design for controlling the molecular packing would be a critical challenge to lower internal reorganization energy. Note that regarding the ligand design and modification it is important that the ligand structure is easy to synthesize and obtain. Our proposal of using transition density as useful theoretical guidance to rationalize substituent effects for reorganization energy would allow one to identify all of the positions suitable for substitutions with minimal impacts on λ_{in} and deactivation rate to provide useful guidelines for the choice of more easily synthesizable ligands.

In addition, Pt(II) complexes with C_{2h} symmetry are expected to preferentially attain face-to-face stacking due to the strong π–π interaction between ligands. In this study, the platinum atoms are located on the z axis both in the ground and excited states. However, as the dimer structure deviates from the fully aligned geometry, the overlap of the d_z^2 orbitals would be decreased and the p_z orbitals of ligands will contribute to σ^* orbitals. Therefore, the transition density also provides information to examine the contribution of ILCT character, which leads to strong vibronic couplings. Further theoretical interpretation of this analytic method, including the impact of the neighboring atoms with bonding and antibonding characters in the transition density and the illustration of porphyrinoids with small internal reorganization energy, is currently under investigation and will be published later.

■ ASSOCIATED CONTENT

Ⓢ Supporting Information

The Supporting Information is available free of charge on the ACS Publications website at DOI: 10.1021/acs.jpcc.9b00224.

> Frontier orbitals, contribution of normal modes to the intramolecular reorganization energy, electrostatic potential, transition density, and bond-length differences for all of the Pt(II) complexes studied in this paper (PDF)

■ AUTHOR INFORMATION

Corresponding Author

*E-mail: yuanchung@ntu.edu.tw.

ORCID

Wei-Chih Chen: 0000-0001-8165-0782

Pi-Tai Chou: 0000-0002-8925-7747

Yuan-Chung Cheng: 0000-0003-0125-4267

Notes

The authors declare no competing financial interest.

■ ACKNOWLEDGMENTS

Y.-C.C. thanks the Ministry of Science and Technology, Taiwan (grant no. MOST 107-2113-M-002-001) and National Taiwan University (grant no. 108L893205) for financial support. We are grateful to the Computer and Information Networking Center, National Taiwan University, for the support of high-performance computing facilities. We are grateful to the National Center for High-Performance Computing for computer time and facilities.

■ REFERENCES

(1) Chou, P.-T.; Chi, Y. Phosphorescent Dyes for Organic Light-Emitting Diodes. *Chem. − Eur. J.* **2007**, *13*, 380−395.

(2) Qian, G.; Wang, Z. Y. Near-Infrared Organic Compounds and Emerging Applications. *Chem. Asian J.* **2010**, *5*, 1006−1029.

(3) Bünzli, J.-C. G.; Eliseeva, S. V. Lanthanide NIR Luminescence for Telecommunications, Bioanalyses and Solar Energy Conversion. *J. Rare Earths* **2010**, *28*, 824−842.

(4) Luo, S. L.; Zhang, E. L.; Su, Y. P.; Cheng, T. M.; Shi, C. M. A Review of NIR Dyes in Cancer Targeting and Imaging. *Biomaterials* **2011**, *32*, 7127−7138.

(5) Guo, Z.; Park, S.; Yoon, J.; Shin, I. Recent Progress in the Development of Near-Infrared Fluorescent Probes for Bioimaging Applications. *Chem. Soc. Rev.* **2014**, *43*, 16−29.

(6) Xiang, H.; Cheng, J.; Ma, X.; Zhou, X.; Chruma, J. J. Near-Infrared Phosphorescence: Materials and Applications. *Chem. Soc. Rev.* **2013**, *42*, 6128−6185.

(7) Lee, T. C.; Hung, J. Y.; Chi, Y.; Cheng, Y. M.; Lee, G. H.; Chou, P. T.; Chen, C. C.; Chang, C. H.; Wu, C. C. Rational Design of Charge-Neutral, Near-Infrared-Emitting Osmium(II) Complexes and OLED Fabrication. *Adv. Funct. Mater.* **2009**, *19*, 2639−2647.

(8) Borisov, S. M.; Nuss, G.; Haas, W.; Saf, R.; Schmuck, M.; Klimant, I. New NIR-Emitting Complexes of Platinum(II) and Palladium(II) with Fluorinated Benzoporphyrins. *J. Photochem. Photobiol., A* **2009**, *201*, 128−135.

(9) Hanson, K.; Tamayo, A.; Diev, V. V.; Whited, M. T.; Djurovich, P. I.; Thompson, M. E. Efficient Dipyrrin-Centered Phosphorescence at Room Temperature from Bis-Cyclometalated Iridium(III) Dipyrrinato Complexes. *Inorg. Chem.* **2010**, *49*, 6077−6084.

(10) Wong, K. M. C.; Yam, V. W. W. Self-Assembly of Luminescent Alkynylplatinum(II) Terpyridyl Complexes: Modulation of Photophysical Properties through Aggregation Behavior. *Acc. Chem. Res.* **2011**, *44*, 424−434.

(11) Rossi, E.; Colombo, A.; Dragonetti, C.; Roberto, D.; Demartin, F.; Cocchi, M.; Brulatti, P.; Fattori, V.; Williams, J. A. G. From Red to Near Infra-Red OLEDs: the Remarkable Effect of Changing from X = -Cl to -NCS in a Cyclometallated [Pt(N^C^N)X] Complex N^C^N = 5-mesityl-1,3-di-(2-pyridyl)benzene. *Chem. Commun.* **2012**, *48*, 3182−3184.

(12) Chung, C. Y.-S.; Li, S. P.-Y.; Louie, M.-W.; Lo, K. K.-W.; Yam, V. W.-W. Induced Self-Assembly and Disassembly of Water-Soluble Alkynylplatinum(II) Terpyridyl Complexes with "Switchable" Near-Infrared (NIR) Emission Modulated by Metal-Metal Interactions over Physiological pH: Demonstration of pH-Responsive NIR Luminescent Probes in Cell-Imaging Studies. *Chem. Sci.* **2013**, *4*, 2453−2462.

(13) Sivchik, V. V.; Grachova, E. V.; Melnikov, A. S.; Smirnov, S. N.; Ivanov, A. Y.; Hirva, P.; Tunik, S. P.; Koshevoy, I. O. Solid-State and Solution Metallophilic Aggregation of a Cationic $[Pt(NCN)L]^+$ Cyclometalated Complex. *Inorg. Chem.* **2016**, *55*, 3351−3363.

(14) Kang, J. J.; Zhang, X. X.; Zhou, H. J.; Gai, X. Q.; Jia, T.; Xu, L.; Zhang, J. J.; Li, Y. Q.; Ni, J. 1-D "Platinum Wire" Stacking Structure Built of Platinum(II) Diimine Bis(sigma-acetylide) Units with Luminescence in the NIR Region. *Inorg. Chem.* **2016**, *55*, 10208−10217.

(15) Prabhath, M. R. R.; Romanova, J.; Curry, R. J.; Silva, S. R. P.; Jarowski, P. D. The Role of Substituent Effects in Tuning Metallophilic Interactions and Emission Energy of Bis-4-(2-pyridyl)-1,2,3-triazolatoplatinum(II) Complexes. *Angew. Chem., Int. Ed.* **2015**, *54*, 7949−7953.

(16) Romanova, J.; Prabhath, M. R. R.; Jarowski, P. D. Relationship between Metallophilic Interactions and Luminescent Properties in Pt(II) Complexes: TD-DFT Guide for the Molecular Design of Light-Responsive Materials. *J. Phys. Chem. C* **2016**, *120*, 2002−2012.

(17) Li, K.; Tong, G. S. M.; Wan, Q. Y.; Cheng, G.; Tong, W. Y.; Ang, W. H.; Kwong, W. L.; Che, C. M. Highly Phosphorescent Platinum(II) Emitters: Photophysics, Materials and Biological Applications. *Chem. Sci.* **2016**, *7*, 1653−1673.

(18) Ly, K. T.; Chen-Cheng, R.-W.; Lin, H.-W.; Shiau, Y.-J.; Liu, S.-H.; Chou, P.-T.; Tsao, C.-S.; Huang, Y.-C.; Chi, Y. Near-Infrared Organic Light-Emitting Diodes with Very High External Quantum Efficiency and Radiance. *Nat. Photonics* **2017**, *11*, 63−68.

(19) Englman, R.; Jortner, J. The Energy Gap Law for Radiationless Transitions in Large Molecules. *Mol. Phys.* **1970**, *18*, 145−164.

(20) Bixon, M.; Jortner, J.; Cortes, J.; Heitele, H.; Michel-Beyerle, M. E. Energy-Gap Law for Nonradiative and Radiative Charge-Transfer in Isolated and in Solvated Supermolecules. *J. Phys. Chem.* **1994**, *98*, 7289−7299.

(21) Peng, Q.; Shi, Q.; Niu, Y.; Yi, Y.; Sun, S.; Li, W.; Shuai, Z. Understanding the Efficiency Drooping of the Deep Blue Organometallic Phosphors: A Computational Study of Radiative and Non-Radiative Decay Rates for Triplets. *J. Mater. Chem. C* **2016**, *4*, 6829−6838.

(22) Shuai, Z. G.; Peng, Q. Organic Light-Emitting Diodes: Theoretical Understanding of Highly Efficient Materials and Development of Computational Methodology. *Natl. Sci. Rev.* **2017**, *4*, No. nww024.

(23) Zhang, X.; Jacquemin, D.; Peng, Q.; Shuai, Z.; Escudero, D. General Approach to Compute Phosphorescent OLED Efficiency. *J. Phys. Chem. C* **2018**, *122*, 6340−6347.

(24) Zhang, Y.; Zhang, Z. X.; Wang, Y.; Li, H.; Bai, F. Q.; Zhang, H. X. The Effect of the Embedded o-carborane Ligand on the Photophysical Properties of a Cyclometalated Pt(II) Complex: A Theoretical Investigation. *Inorg. Chem. Front.* **2018**, *5*, 1016−1025.

(25) Wang, Y.; Bao, P.; Wang, J.; Jia, R.; Bai, F. Q.; Zhang, H. X. Comprehensive Investigation into Luminescent Properties of Ir(III) Complexes: An Integrated Computational Study of Radiative and Nonradiative Decay Processes. *Inorg. Chem.* **2018**, *57*, 6561−6570.

(26) Strouse, G. F.; Schoonover, J. R.; Duesing, R.; Boyde, S.; Jones, W. E., Jr.; Meyer, T. J. Influence Of Electronic Delocalization In Metal-to-Ligand Charge Transfer Excited States. *Inorg. Chem.* **1995**, *34*, 473−487.

(27) Kui, S. F.; Sham, I. T.; Cheung, C. C.; Ma, C. W.; Yan, B.; Zhu, N.; Che, C. M.; Fu, W. F. Platinum(II) Complexes with π-Conjugated, Naphthyl-Substituted, Cyclometalated Ligands (RC^N^N): Structures and Photo- and Electroluminescence. *Chem. − Eur. J.* **2007**, *13*, 417−435.

(28) Tong, G. S. M.; Che, C. M. Emissive or Nonemissive? A Theoretical Analysis of the Phosphorescence Efficiencies of Cyclometalated Platinum(II) Complexes. *Chem. − Eur. J.* **2009**, *15*, 7225−7237.

(29) Rausch, A. F.; Murphy, L.; Williams, J. A. G.; Yersin, H. Improving the Performance of Pt(II) Complexes for Blue Light Emission by Enhancing the Molecular Rigidity. *Inorg. Chem.* **2012**, *51*, 312−319.

(30) Prokhorov, A. M.; Hofbeck, T.; Czerwieniec, R.; Suleymanova, A. F.; Kozhevnikov, D. N.; Yersin, H. Brightly Luminescent Pt(II) Pincer Complexes with a Sterically Demanding Carboranyl-Phenylpyridine Ligand: A New Material Class for Diverse Optoelectronic Applications. *J. Am. Chem. Soc.* **2014**, *136*, 9637−9642.

(31) Chang, S. Y.; Kavitha, J.; Li, S. W.; Hsu, C. S.; Chi, Y.; Yeh, Y. S.; Chou, P. T.; Lee, G. H.; Carty, A. J.; Tao, Y. T.; et al. Platinum(II) Complexes with Pyridyl Azolate-Based Chelates: Synthesis, Structural Characterization, and Tuning of Photo- and Electrophosphorescence. *Inorg. Chem.* **2006**, *45*, 137−146.

(32) Kim, K. H.; Liao, J. L.; Lee, S. W.; Sim, B.; Moon, C. K.; Lee, G. H.; Kim, H. J.; Chi, Y.; Kim, J. J. Crystal Organic Light-Emitting Diodes with Perfectly Oriented Non-Doped Pt-Based Emitting Layer. *Adv. Mater.* **2016**, *28*, 2526−2532.

(33) Frisch, M. J.; Trucks, G. W.; Schlegel, H. B.; Scuseria, G. E.; Robb, M. A.; Cheeseman, J. R.; Scalmani, G.; Barone, V.; Mennucci, B.; Petersson, G. A. et al. *Gaussian 09*, revision D.01; Gaussian Inc.: Wallingford, CT, 2013.

(34) Grimme, S.; Ehrlich, S.; Goerigk, L. Effect of the Damping Function in Dispersion Corrected Density Functional Theory. *J. Comput. Chem.* **2011**, *32*, 1456−1465.

(35) Grimme, S. Density Functional Theory with London Dispersion Corrections. *WIREs Comput. Mol. Sci.* **2011**, *1*, 211−228.

(36) Zhou, X.; Zhang, H. X.; Pan, Q. J.; Li, M. X.; Wang, Y.; Che, C. M. Electronic Structures and Spectroscopic Properties of $[\mathrm{Pt(CNMe)_2(CN)_2}]_n$ (n = 1-4): A Theoretical Exploration of Promising Phosphorescent Materials. *Eur. J. Inorg. Chem.* **2007**, 2181−2188.

(37) Bai, F. Q.; Zhou, X.; Xia, B. H.; Liu, T.; Zhang, J. P.; Zhang, H. X. Electronic Structures and Optical Properties of Neutral Substituted Fluorene-Based Cyclometalated Platinum(II)-Acetylide Complexes: A DFT Exploration. *J. Organomet. Chem.* **2009**, *694*, 1848−1860.

(38) Niehaus, T. A.; Hofbeck, T.; Yersin, H. Charge-Transfer Excited States in Phosphorescent Organo-Transition Metal Compounds: A Difficult Case for Time Dependent Density Functional Theory? *RSC Adv.* **2015**, *5*, 63318−63329.

(39) Kim, D.; Brédas, J. L. Triplet Excimer Formation in Platinum-Based Phosphors: A Theoretical Study of the Roles of Pt-Pt Bimetallic Interactions and Interligand π-π Interactions. *J. Am. Chem. Soc.* **2009**, *131*, 11371−11380.

(40) Peach, M. J. G.; Williamson, M. J.; Tozer, D. J. Influence of Triplet Instabilities in TDDFT. *J. Chem. Theory Comput.* **2011**, *7*, 3578−3585.

(41) Sears, J. S.; Koerzdoerfer, T.; Zhang, C. R.; Brédas, J. L. Communication: Orbital Instabilities and Triplet States from Time-Dependent Density Functional Theory and Long-Range Corrected Functionals. *J. Chem. Phys.* **2011**, *135*, No. 151103.

(42) Brédas, J.-L.; Beljonne, D.; Coropceanu, V.; Cornil, J. Charge-Transfer and Energy-Transfer Processes in π-Conjugated Oligomers and Polymers: A Molecular Picture. *Chem. Rev.* **2004**, *104*, 4971−5003.

(43) Coropceanu, V.; Cornil, J.; da Silva Filho, D. A.; Olivier, Y.; Silbey, R.; Brédas, J. L. Charge Transport in Organic Semiconductors. *Chem. Rev.* **2007**, *107*, 926−952.

(44) Shuai, Z.; Geng, H.; Xu, W.; Liao, Y.; Andre, J.-M. From Charge Transport Parameters to Charge Mobility in Organic Semiconductors through Multiscale Simulation. *Chem. Soc. Rev.* **2014**, *43*, 2662−2679.

(45) Albright, T. A.; Burdett, J. K.; Whangbo, M. H. *Orbital Interactions in Chemistry*; John Wiley & Sons: New York, 1985.

(46) Wysokiński, R.; Michalska, D. The Performance of Different Density Functional Methods in the Calculation of Molecular Structures and Vibrational Spectra of Platinum(II) Antitumor Drugs: Cisplatin and Carboplatin. *J. Comput. Chem.* **2001**, *22*, 901−912.

(47) Wysokiński, R.; Hernik, K.; Szostak, R.; Michalska, D. Electronic Structure and Vibrational Spectra of cis-diammine-(orotato)platinum(II), A Potential Cisplatin Analogue: DFT and Experimental Study. *Chem. Phys.* **2007**, *333*, 37−48.

(48) Kato, T.; Yamabe, T. Vibronic Interactions and Superconductivity in Acene Anions and Cations. *J. Chem. Phys.* **2001**, *115*, 8592−8602.

(49) Kwon, O.; Coropceanu, V.; Gruhn, N. E.; Durivage, J. C.; Laquindanum, J. G.; Katz, H. E.; Cornil, J.; Brédas, J. L. Characterization of the Molecular Parameters Determining Charge Transport in Anthradithiophene. *J. Chem. Phys.* **2004**, *120*, 8186−8194.

(50) Chen, H. Y.; Chao, I. Effect of Perfluorination on the Charge-Transport Properties of Organic Semiconductors: Density Functional Theory Study of Perfluorinated Pentacene and Sexithiophene. *Chem. Phys. Lett.* **2005**, *401*, 539−545.

(51) Kuo, M. Y.; Chen, H. Y.; Chao, I. Cyanation: Providing a Three-in-One Advantage for the Design of n-Type Organic Field-Effect Transistors. *Chem. − Eur. J.* **2007**, *13*, 4750−4758.

(52) Chang, Y. C.; Chao, I. An Important Key to Design Molecules with Small Internal Reorganization Energy: Strong Nonbonding Character in Frontier Orbitals. *J. Phys. Chem. Lett.* **2010**, *1*, 116−121.

(53) Chen, W. C.; Chao, I. Molecular Orbital-Based Design of π-Conjugated Organic Materials with Small Internal Reorganization Energy: Generation of Nonbonding Character in Frontier Orbitals. *J. Phys. Chem. C* **2014**, *118*, 20176−20183.

(54) Dreuw, A.; Head-Gordon, M. Single-Reference ab Initio Methods for the Calculation of Excited States of Large Molecules. *Chem. Rev.* **2005**, *105*, 4009−4037.

(55) Grimme, S.; Djukic, J. P. Cation-Cation "Attraction": When London Dispersion Attraction Wins over Coulomb Repulsion. *Inorg. Chem.* **2011**, *50*, 2619−2628.

(56) Thiel, D. J.; Livins, P.; Stern, E. A.; Lewis, A. Microsecond-Resolved XAFS of the Triplet Excited-State of $\mathrm{Pt_2(P_2O_5H_2)_4^{4-}}$. *Nature* **1993**, *362*, 40−43.

(57) Novozhilova, I. V.; Volkov, A. V.; Coppens, P. Theoretical Analysis of the Triplet Excited State of the $[\mathrm{Pt_2(H_2P_2O_5)_4}]^{4-}$ Ion and Comparison with Time-Resolved X-ray and Spectroscopic Results. *J. Am. Chem. Soc.* **2003**, *125*, 1079−1087.

(58) van der Veen, R. M.; Milne, C. J.; El Nahhas, A.; Lima, F. A.; Pham, V. T.; Best, J.; Weinstein, J. A.; Borca, C. N.; Abela, R.; Bressler, C.; et al. Structural Determination of a Photochemically Active Diplatinum Molecule by Time-Resolved EXAFS Spectroscopy. *Angew. Chem. Int. Ed.* **2009**, *48*, 2711−2714.

(59) Lockard, J. V.; Rachford, A. A.; Smolentsev, G.; Stickrath, A. B.; Wang, X. H.; Zhang, X. Y.; Atenkoffer, K.; Jennings, G.; Soldatov, A.; Rheingold, A. L.; et al. Triplet Excited State Distortions in a Pyrazolate Bridged Platinum Dimer Measured by X-Ray Transient Absorption Spectroscopy. *J. Phys. Chem. A* **2010**, *114*, 12780−12787.

(60) Christensen, M.; Haldrup, K.; Kjaer, K. S.; Cammarata, M.; Wulff, M.; Bechgaard, K.; Weihe, H.; Harrit, N. H.; Nielsen, M. M. Structure of a Short-Lived Excited State Trinuclear Ag-Pt-Pt Complex in Aqueous Solution by Time Resolved X-Ray Scattering. *Phys. Chem. Chem. Phys.* **2010**, *12*, 6921−6923.

(61) Cho, Y. J.; Kim, S. Y.; Son, H. J.; Cho, D. W.; Kang, S. O. Steric Effect on Excimer Formation in Planar Pt(II) Complexes. *Phys. Chem. Chem. Phys.* **2017**, *19*, 5486−5494.

(62) Milota, F.; Prokhorenko, V. I.; Mancal, T.; von Berlepsch, H.; Bixner, O.; Kauffmann, H. F.; Hauer, J. Vibronic and Vibrational Coherences in Two-Dimensional Electronic Spectra of Supramolecular J-Aggregates. *J. Phys. Chem. A* **2013**, *117*, 6007−6014.

DOI: 10.1021/acs.jpcc.9b00224
J. Phys. Chem. C 2019, 123, 10225−10236